Three-dimensional computed tomography confirmed that the meniscal root attachments and meniscofemoral ligaments are morphologically consistent

Koh Tanifuji, Goro Tajima, Jun Yan, Moritaka Maruyama, Atsushi Sugawara, Shinya Oikawa, Ryunosuke Oikawa, Sho Kikuchi & Minoru Doita

ONLINE FIRST

Knee Surgery, Sports Traumatology, Arthroscopy

ISSN 0942-2056

Knee Surg Sports Traumatol Arthrosc
DOI 10.1007/s00167-020-06095-1

Knee Surgery, Sports Traumatology, Arthroscopy
https://doi.org/10.1007/s00167-020-06095-1

KNEE

Three-dimensional computed tomography confirmed that the meniscal root attachments and meniscofemoral ligaments are morphologically consistent

Koh Tanifuji[1] · Goro Tajima[1] · Jun Yan[2] · Moritaka Maruyama[1] · Atsushi Sugawara[1] · Shinya Oikawa[1] · Ryunosuke Oikawa[1] · Sho Kikuchi[1] · Minoru Doita[1]

Received: 3 February 2020 / Accepted: 10 June 2020

Abstract

Purpose To clarify the characteristic features of the meniscal root attachments, meniscofemoral ligaments (MFLs), and related osseous landmarks on three-dimensional images using computed tomography.

Methods Twenty-eight non-paired, formalin-fixed human cadaveric knees were evaluated in this study. The meniscal root attachments were identified and marked. Three-dimensional images were obtained after applying a contrast agent to the entire meniscal surfaces and MFLs, then the morphology of the meniscal root attachments and MFLs, and their positional relationships with osseous landmarks, were analyzed.

Results Parsons' knob divided the medial meniscal anterior root attachment and lateral meniscal anterior root attachment on the anterior portion of the tibial plateau. The medial meniscal posterior root attachment was near the medial intercondylar tubercle. The lateral meniscal posterior root attachment (LMPRA) was closer to the lateral intercondylar tubercle. Both root attachments were near the posterior intercondylar fossa. The positional relationships between the meniscal root attachments and related osseous landmarks were consistent in all specimens. The MFLs originated from the lateral meniscus posterior horn, and the anterior MFL was closer to the LMPRA than the posterior MFL. The posterior MFL originated at approximately the midpoint between the LMPRA and the most posterior margin of the lateral meniscus.

Conclusion This study showed that the relationships between the characteristic features of the meniscal root attachments, MFLs, and related osseous landmarks were consistent. The clinical relevance of this study is that it improved understanding of the anatomy of the meniscal root attachments and MFLs.

Keywords Meniscal root attachments · Meniscofemoral ligaments · Knee · Three-dimensional computed tomography

Abbreviations

MMARA	Medial meniscal anterior root attachment
LMARA	Lateral meniscal anterior root attachment
MMPRA	Medial meniscal posterior root attachment
LMPRA	Lateral meniscal posterior root attachment
MIT	Medial intercondylar tubercle
LIT	Lateral intercondylar tubercle
PIF	Posterior intercondylar fossa
MFLs	Meniscofemoral ligaments
aMFL	Anterior meniscofemoral ligament
pMFL	Posterior meniscofemoral ligament
3D	Three-dimensional
CT	Computed tomography

✉ Goro Tajima
gorot@iwate-med.ac.jp

1 Department of Orthopedic Surgery, Iwate Medical University, 2-1-1, Idaidori, Yahaba, Iwate, Japan

2 Department of Anatomy, Iwate Medical University, 2-1-1, Idaidori, Yahaba, Iwate, Japan

Introduction

The menisci play important roles in load-bearing and shock-absorbing in the tibiofemoral joint, and increase the surface areas for load transmission [1, 15, 16, 18, 26]. During load transmission, the forces acting on the menisci are transformed into circumferential hoop stress, which is transmitted to the tibial plateau by the anterior and posterior meniscal roots [23]. Furthermore, the posterior horn of the lateral meniscus is connected to the intercondylar area of the femur by the meniscofemoral ligaments (MFLs), which consist of

Published online: 20 June 2020

the anterior MFL (aMFL) and posterior MFL (pMFL) and which plays a functional role in resisting posterior drawer and stabilizing the lateral meniscus [8, 10, 31].

Meniscal root tears lead to severe functional failure of the menisci to convert axial loads into transverse hoop stress, which can result in an increased risk of osteoarthritis and osteonecrosis [19, 25]. Medial meniscal posterior root tears are mainly the result of degenerative meniscal disease and are frequently found in middle-aged women, in Asian patients [4, 11]. In contrast, lateral meniscal posterior root tears are usually traumatic in nature and have been reported in 7–12% of patients with anterior cruciate ligament (ACL) injuries [2, 3]. Few clinical reports discuss solitary injuries to the MFLs, and whether intact MFLs influence increasing mean contact pressure in the lateral compartment with lateral meniscal posterior root tears [5, 8]. Numerous surgical treatments for meniscal root tears have been reported [17, 20, 30]. Recently, the transtibial pull-out repair and the suture anchor techniques have been used commonly as surgical options to preserve important meniscal functions [21]. It has been widely reported that placing the meniscal root attachments in their proper anatomical locations is critical to restoring meniscal function [9, 22, 28].

Creating a bone tunnel or a drill hole to repair the meniscal root attachments and place them in a physiological position is a technically complicated procedure, including the use of the necessary instruments. In particular, the posterior tibiofemoral space is extremely narrow, depending on the patient, and inaccurate bone tunnel or drill hole placement may lead to potential injuries to other normal structures [28]. More anatomical, and safer and exact root repair techniques would be ensured by understanding the detailed morphology of the meniscal root attachments. However, few studies evaluated the actual positions of the meniscal root attachments and MFLs and their positional relationships with osseous landmarks [13, 14].

The aim of the present study was to clarify the characteristic features of the meniscal root attachments, MFLs, and related osseous landmarks on three-dimensional (3D) computed tomography (CT) images. Our hypothesis was that definable and consistent identification of the meniscal root attachments and MFLs in relation to arthroscopically pertinent osseous landmarks was possible.

Materials and methods

Twenty-eight unpaired human cadaveric knees (12 from male cadavers and 16 from female cadavers), with no severe macroscopic degenerative or traumatic changes were used in the present study. The mean age at the time of death was 82.0 ± 8.8 years (range, 63–89 years). All cadavers were placed in 10% formalin and preserved in 50% alcohol for 6 months. The cadavers were donated to Iwate Medical University for education and research purposes, and informed consent for donation was obtained from each patient and their family prior to death. This cadaveric study was approved by the Ethical Committee of Iwate Medical University (IRB: H27-99).

Dissection was begun by excising the left knee from the distal femur and the proximal tibia and fibula from the specimen and removing the skin and soft tissues around the knee. After the articular capsule was exposed, it was gently peeled off the menisci to identify the medial and lateral menisci and the MFLs. The femur was divided longitudinally with the long axis, and the lateral femoral condyle and the ACL were excised. Then, the MFLs and PCL were observed grossly. After identification, the femur, MFLs, and the PCL were excised, and the meniscal root structures underwent detailed dissection to accurately identify them. Next, the meniscal root attachments were outlined by manually inserting fine 0.5-mm pins into their margins at intervals of approximately 3 mm.

3D visualization and measurements

After carefully painting the entire meniscal surfaces and MFLs with a contrast agent (Iopamiron 300; Bayer Yakuhin Ltd., Osaka, Japan) to distinguish them because the cartilage of the tibial plateau, menisci, and MFLs have similar CT values, all knees were scanned using a 16-row multislice CT scanner (ECLOS; Hitachi Medical Corporation, Tokyo, Japan). Axial plane images with 0.5-mm slices were obtained and saved as Digital Imaging and Communications in Medicine data. All data were uploaded to dedicated software (Mimics version 21.0; Materialise NV, Leuven, Belgium), and accurate 3D images of the specimens, including each segment of the bone, ligaments, and menisci were created. A segmentation technique was then applied to each CT density mask to identify and separate the menisci by differences in density from the tibia and surrounding residual soft tissue using specific software. The data from the 3D images were uploaded to an advanced analysis software (3-matic version 15.0; Materialise NV).

The characteristic features of the meniscal root attachments, MFLs, and related osseous structures such as Parsons' knob, the medial and lateral intercondylar tubercles (MIT, LIT), and the posterior intercondylar fossa (PIF) and their positional relationships were analyzed on the 3D images. The centers of the attachments were automatically defined as the center of their surfaces by the software. The apices of the MIT and LIT, and the anteromedial and anterolateral corners of the PIF were similarly defined. The coordinates of the centers of the attachments were mapped on coordinate grids on the tibial plane from the 3D images, with the 3D measurements made according to the method described by Tajima et al. [29]. Regarding the characteristic features of the meniscal origin of the pMFL, the positional relationships between the lateral meniscal posterior root attachment (LMPRA) and the most posterior margin of the lateral meniscus were examined using the software. Data for the aMFL were excluded from this study because the prevalence of the aMFL was extremely low in our cadavers.

The accuracy of the length and area measurements was within < 0.1 mm and 0.1 mm^2, respectively. When comparing the accuracy of the 3D CT images with the optical scans, the average error was 0.65 ± 0.31 mm or approximately one-third of the pixel size [7]. The tolerance and margin of error for the CT measurements (according to the manufacturer) were both ± 0.39 mm. The distribution of each variable was checked for normality using the Kolmogorov–Smirnov test, and all statistical data were analyzed using SPSS v.22.0 (IBM Corporation; Armonk, NY, USA).

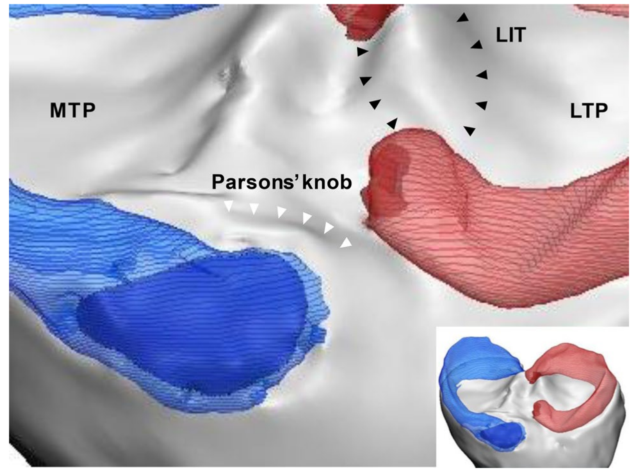

Fig. 1 Characteristic features of the meniscal anterior root attachments and related osseous structures on 3D images superoanterior view. The blue and red transparent areas indicate the medial meniscus and lateral meniscus, and the blue and red areas indicate the MMARA and LMARA, respectively. The white arrowheads indicate Parsons' knob, and the black arrowheads indicate the LIT. *3D* three-dimensional, *MTP* medial tibial plateau, *LTP* lateral tibial plateau, *LIT* lateral intercondylar tubercle, *MMARA* medial meniscal anterior root attachment, *LMARA* lateral meniscal anterior root attachment

Results

Characteristic features of the meniscal root attachments and related osseous structures on 3D images

The medial meniscal anterior root attachment (MMARA) had a broad semicircular shape and was located on the most anterior portion of the tibial plateau. The MMARA attached to the slope, which was on the anterior intercondylar crest and consisted of the anterior slope of Parsons' knob, the anterolateral edge of the medial tibial plateau continuous from Parsons' knob, and the anterior edge of the tibia (Fig. 1). The lateral meniscal anterior root attachment (LMARA) was a relatively compact oval shape located anteromedial to the LIT, posterior to Parsons' knob, and lateral to the ACL. The medial side of the LMARA partially overlapped the ACL tibial insertion site (Fig. 1). The medial meniscal posterior root attachment (MMPRA) and the LMPRA were also oval-shaped. The MMPRA attached to the posterior portion of the tibial plateau adjacent to the PCL. The MMPRA was surrounded by the posterior side of the MIT, lateral edge of the medial tibial plateau, and anteromedial edge of the PIF where the PCL attaches to the tibia (Fig. 2). The LMPRA was located on the center of the medial wall of the LIT, posteromedial to the tubercle's apex, and near the anterolateral edge of the PIF (Fig. 2). A few fibers made up the LMPRA, which continued toward the lateral wall of the MIT. Quantitative data are summarized in Table 1.

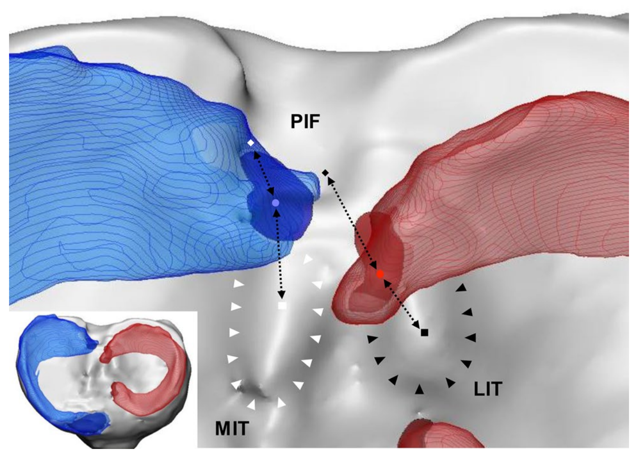

Fig. 2 Characteristic features of the meniscal posterior root attachments and related osseous structures on 3D images superior view. The blue and red transparent areas indicate the medial meniscus and lateral meniscus, and the blue and red areas indicate the MMPRA and LMPRA, respectively. The white arrowheads indicate the MIT, and the black arrowheads indicate the LIT. The white square indicates the apex of the MIT, and the black square indicates the apex of the LIT. The white rhombus indicates the anteromedial corner of the PIF, and the black rhombus indicates the anterolateral corner of the PIF. The blue circle indicates the center of the MMPRA, and the red circle indicates the center of the LMPRA. *3D* three-dimensional, *MMPRA* medial meniscal posterior root attachment, *LMPRA* lateral meniscal posterior root attachment, MIT medial intercondylar tubercle, LIT lateral intercondylar tubercle, PIF posterior intercondylar fossa

Table 1 Quantitative measurements of the meniscal root attachments and related osseous landmarks

Distance from the MMPRA (mm)	
To the apex of the MIT	9.3 ± 1.5 (6.1–12.4)
To the anteromedial corner of the PIF	6.2 ± 1.1 (3.4–7.9)
Distance from the LMPRA (mm)	
To the apex of the LIT	6.9 ± 2.0 (3.4–12.2)
To the anterolateral corner of the PIF	11.1 ± 1.3 (9.1–13.0)
Mean surface area (mm^2)	
MMARA	117.1 ± 31.4 (79.0–184.8)
LMARA	32.3 ± 12.1 (14.0–59.4)
MMPRA	50.8 ± 16.9 (33.8–78.0)
LMPRA	28.7 ± 13.5 (11.0–59.0)

Data are presented as mean ± standard deviation (range)

MMPRA medial meniscal posterior root attachment, *LMPRA* lateral meniscal posterior root attachment, *MMARA* medial meniscal anterior root attachment, *LMARA* lateral meniscal anterior root attachment, *MIT* medial intercondylar tubercle, *PIF* posterior intercondylar fossa, *LIT* lateral intercondylar tubercle

Coordinate positions of the centers of the meniscal root attachments on the 3D images

The centers of the lateral meniscal root attachments were located more centrally than the medial meniscal root attachments anteroposteriorly, and all the centers of the meniscal root attachments were located approximately 10% further from the center mediolaterally. Figure 3 is a 3D image of the tibial plateau. A grid was overlaid indicating 0–100% of the distance across the plateau extending laterally and posteriorly from the anteromedial corner of the plateau. Quantitative data are summarized in Table 2.

Prevalence of the MFLs and characteristic features of the meniscal origin of the pMFL on 3D images

The prevalence of the aMFL and pMFL was 21.4% and 85.7%, respectively, and 17.9% of the knees had both ligaments. The MFLs originated from the lateral margin of the lateral meniscus posterior horn, and the aMFL was closer to the LMPRA than the pMFL (Fig. 4). The MFLs extended to the medial wall of the femoral intercondylar notch, and embraced the PCL at the intersection with the MFLs. Differences in the fiber orientations between the MFLs were found. Regarding the characteristic features of the meniscal origin of the pMFL, the distance from the LMPRA to the most posterior margin of the lateral meniscus (ac) was 19.0 mm, the distance from the LMPRA to the meniscal origin of the pMFL (ab) was 9.0 mm, and the ratio between the two distances (ab/ac) was 47.7% (Fig. 5). Quantitative data are summarized in Table 3.

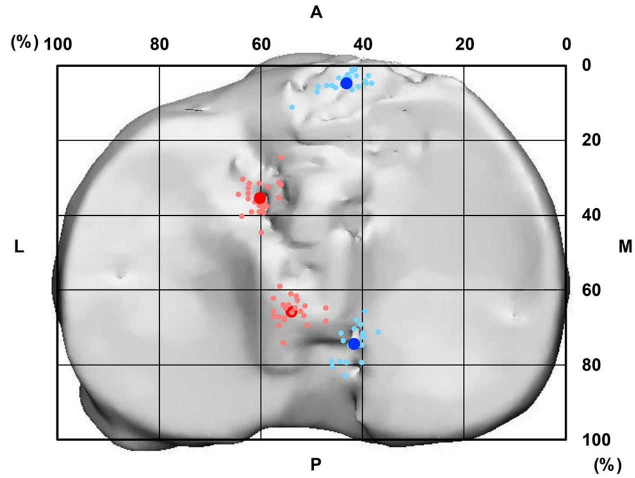

Fig. 3 Coordinate positions of the centers of the meniscal root attachments on 3D images. In a true proximal to distal view of the tibial plateau, a rectangle was fitted based on the most posterior margins of the medial and lateral tibial condyles. The sides constituting the rectangle were in contact with the anteroposterior and mediolateral edges of the tibial plateau. The anteroposterior and mediolateral axes were defined according to the anteromedial corner of the rectangle, and the coordinate axes, indicated by percentage ratios, were created. The centers of the meniscal root attachments were projected on the coordinate axes on the tibial plane, vertically. Coordinates for the centers of the medial meniscal root attachments (small blue dots) and lateral meniscal root attachments (small red dots) are shown, and the large blue and red dots indicate the mean centers of the respective attachments. *3D* three-dimensional

Discussion

The most important results in the present study were the visualization and clarification of the characteristic features of the meniscal root attachments, MFLs, and their related osseous landmarks on 3D CT images. The varying regional morphology of the relationships between the meniscal attachments and the osseous landmarks had intrinsic features in each portion. Regarding the morphology of the MFLs, the locations of the meniscal origin of the pMFL and the LMPRA were consistent. Our understanding of the anatomy of the meniscal root attachments and MFLs was improved by these findings, which may assist surgeons in performing anatomical procedures to treat meniscal root tears.

This study provided novel important findings that the positional relationships between the meniscal root attachments and osseous landmarks were consistent, with low standard deviations. This study showed that Parsons' knob, which divided the MMARA and LMARA, was an important osseous landmark regarding the anterior root attachments of the menisci. Furthermore, the apices of the MIT and LIT, and anteromedial and anterolateral corners of the PIF were shown to be adjacent to the MMPRA and LMPRA. Johannsen et al. reported that the MIT, LIT, tibial plateau

Table 2 Locations of the centers of the meniscal root attachments on 3D images

(%)	From the anterior edge of the tibia	From the medial edge of the tibia
MMARA	4.6 ± 2.2 (1.3–11.4)	43.4 ± 3.6 (38.3–53.9)
LMARA	35.6 ± 4.2 (24.7–45.0)	60.2 ± 2.4 (56.1–64.4)
MMPRA	74.4 ± 4.2 (65.8–83.1)	41.8 ± 2.2 (36.9–46.2)
LMPRA	65.7 ± 3.2 (59.1–74.4)	54.0 ± 2.8 (47.3–57.6)

Data are presented as mean ± standard deviation (range) and indicate the percentage distance from the indicated edge with a range of 0–100% extending laterally and posteriorly from the anteromedial corner of the tibial plateau

3D three-dimensional, *MMARA* medial meniscal anterior root attachment, *LMARA* lateral meniscal anterior root attachment, *MMPRA* medial meniscal posterior root attachment, *LMPRA* lateral meniscal posterior root attachment

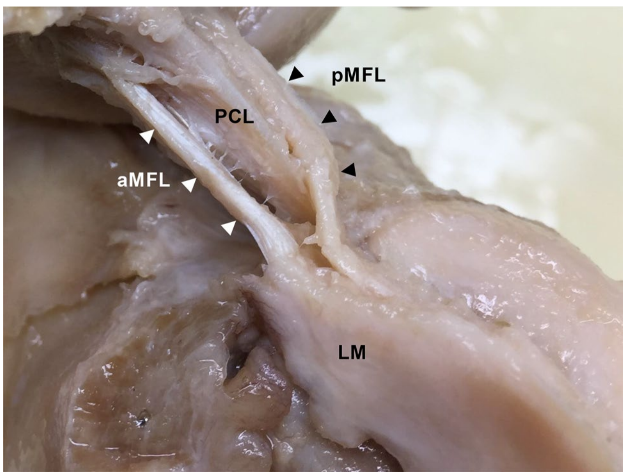

Fig. 4 Macroscopic findings in a superolateral view of the left knee showing the meniscal origin of the MFLs. The MFLs consist of the aMFL (white arrowheads) and the pMFL (black arrowheads), which runs across the PCL. *MFL* meniscofemoral ligament, *aMFL* anterior MFL, *pMFL* posterior MFL, *PCL* posterior cruciate ligament, *LM* lateral meniscus

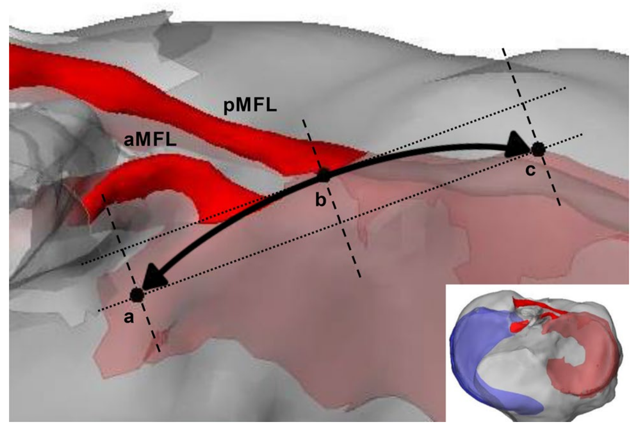

Fig. 5 Characteristic features of the meniscal origin of the pMFL on 3D images. Points a, b, and c indicate the LMPRA, the meniscal origin of the pMFL, and the most posterior margin of the lateral meniscus, respectively. *3D* three-dimensional, *aMFL* anterior meniscofemoral ligament, *pMFL* posterior meniscofemoral ligament, *LMPRA* lateral meniscal posterior root attachment

articular cartilage edge, and the PCL tibial attachment were useful landmarks for the MMPRA and LMPRA in their cadaveric studies [12]. In a CT and magnetic resonance imaging (MRI) study, Fujii et al. reported that the posterior dimple that is present in the PIF was an osseous landmark for the MMPRA and the PCL tibial attachment; however, the authors did not qualitatively analyze these structures' positional relationships, and stated that it might be difficult to confirm the posterior dimple, intraoperatively [6]. Sheps et al. and Tajima et al. identified the anatomical characteristics of the PIF with anatomical reference points representing the corners, which can be found consistently, visually or by palpation [27, 29]. In this study, the relationships between the meniscal posterior root attachments and their osseous landmarks that can be identified arthroscopically were clearly visualized and qualitatively examined, providing clinically useful findings for surgeons performing arthroscopic meniscal root repairs.

Table 3 Quantitative measurements of the meniscal origin of the pMFL

Distances	
From the LMPRA (a), (mm)	
To the meniscal origin of the pMFL (b)	9.0 ± 2.2 (6.5–14.2)
To the most posterior margin of the LM (c)	19.0 ± 2.8 (14.3–25.5)
Ratio of distance ab to distance ac, (%)	47.7 ± 9.3 (31.8–70.0)

Data are presented as mean ± standard deviation (range)

pMFL posterior meniscofemoral ligament, *LMPRA* lateral meniscal posterior root attachment, *LM* lateral meniscus

The accurate coordinate positions of the centers of the meniscal root attachments on the tibial plateau were determined using 3D images, in this study. The mapping measurement method used in this study has several advantages compared with previous studies. The method provided the measurements as a percentage of the actual length of the tibial plateau, enabling us to minimize the influence of individual differences [24]. Furthermore, 3D CT data are directly and accurately translatable to standard CT as a functional specification of this imaging modality [24]. Therefore, measurements on 3D images are useful for preoperative planning, postoperative evaluation of the tunnel position using CT or MRI, as well as for intraoperatively determining the tunnel position when using fluoroscopy or a navigation system.

In particular, this study revealed the characteristic features of the meniscal origin of the pMFL. The anatomy of the MFLs has been described by several authors; however, almost all reports focused on the morphological variations in the MFLs or their femoral attachments. The pMFL originated at approximately the midpoint between the LMPRA and the most posterior margin of the lateral meniscus, in this study. Forkel et al. reported in a biomechanical study, that LMPRA tears combined with MFL injury resulted in a significant increase in tibiofemoral contact pressure, indicating that the biomechanical consequences of LMPRA tears depend on MFL status [5]. Clinically, when lateral meniscal tears occur between the LMPRA and the meniscal origin of the pMFL, the pMFL might remain intact. Therefore, it is believed that our findings will be useful for predicting lateral meniscal instability by assessing the location of the LMPRA tear, and might contribute to decisions regarding the indications for a lateral meniscal root repair.

Our study had several limitations. First, the cadavers had a high mean age. Even though no specimens had severe macroscopic degenerative or traumatic changes, degenerative changes may have affected identifying the osseous landmarks. Second, a relatively small number of specimens was evaluated. Third, although an accurate 3D measurement method was used in this study, human dissection and subjective decisions regarding the meniscal root attachments and MFLs may have introduced error and bias. Fourth, formalin-preserved cadavers were used, in which it is occasionally difficult to identify detailed soft tissue structures.

The clinical relevance of this study is that it improved understanding of the anatomy of the meniscal root attachments and MFLs, which may assist surgeons when performing precise anatomical repairs of the meniscal root attachments.

Conclusion

The relationships between the characteristic features of the meniscal root attachments, MFLs, and related osseous landmarks were consistent, using 3D images. The clinical relevance of this study is that understanding of the anatomy of the meniscal root attachments and MFLs was improved, and our findings may assist surgeons performing exact anatomical repairs of these structures.

Acknowledgements This work was supported by JSPS KAKENHI Grant No. 20K11310. The authors wish to thank Professors Jiro Hitomi, Yoichi Sato and Tomoyuki Saino from the Department of Anatomy of Iwate Medical University for their continuous support of this study. We also thank Mr. Masayoshi Kamata from the Department of Radiology of Iwate Medical University Hospital for his technical assistance. We thank Jane Charbonneau, DVM, from Edanz Group (www.edanzediting.com/ac) for editing a draft of this manuscript.

Compliance with ethical standards

Funding This work was supported by Japan Society for the Promotion of Science KAKENHI [grant number 20K11310].

Conflict of interest All authors declare that they have no conflict of interest.

Ethical approval All procedures performed in studies involving human participants were in accordance with ethical standards of the institutional and/or national research committee and with the 1964 Helsinki declaration and its later amendments or comparable standards. This cadaveric study was approved by the Ethical Committee of Iwate Medical University (IRB: H27-99).

Informed consent Informed consent was obtained from the families of the donors included in this study.

References

1. Ahmed AM, Burke DL (1983) In-vitro measurement of static pressure distribution in synovial joints—Part I: tibial surface of the knee. J Biomech Eng 105:216–225
2. Ahn JH, Lee YS, Yoo JC, Chang MJ, Park SJ, Pae YR (2010) Results of arthroscopic all-inside repair for lateral meniscus root tear in patients undergoing concomitant anterior cruciate ligament reconstruction. Arthroscopy 26:67–75
3. Anderson L, Watts M, Shapter O, Logan M, Risebury M, Duffy D, Myers P (2010) Repair of radial tears and posterior horn detachments of the lateral meniscus: minimum 2-year follow-up. Arthroscopy 26:1625–1632
4. Bae JH, Paik NH, Park GW, Yoon JR, Chae DJ, Kwon JH, Kim JI, Nha KW (2013) Predictive value of painful popping for a posterior root tear of the medial meniscus in middle-aged to older Asian patients. Arthroscopy 29:545–549
5. Forkel P, Herbort M, Schulze M, Rosenbaum D, Kirstein L, Raschke M, Petersen W (2013) Biomechanical consequences of a posterior root tear of the lateral meniscus: stabilizing effect of the meniscofemoral ligament. Arch Orthop Trauma Surg 133:621–626
6. Fujii M, Furumatsu T, Miyazawa S, Kodama Y, Hino T, Kamatsuki Y, Ozaki T (2017) Bony landmark between the attachment of the medial meniscus posterior root and the posterior cruciate ligament: CT and MR imaging assessment. Skeletal Radiol 46:1041–1045
7. Gelaude F, Vander Sloten J, Lauwers B (2008) Accuracy assessment of CT-based outer surface femur meshes. Comput Aided Surg 13:188–199

8. Gupte CM, Bull AMJ, Thomas RD, Amis AA (2003) The meniscofemoral ligaments: secondary restraints to posterior drawer. J Bone Joint Surg Br 85:765–773
9. Harner CD, Mauro CS, Lesniak BP, Romanowski JR (2009) Biomechanical consequences of a tear of the posterior root of the medial meniscus. J Bone Joint Surg Am 91(Suppl 2):257–270
10. Heller L, Langman J (1964) The menisco-femoral ligaments of the human knee. J Bone Joint Surg Br 46:307–313
11. Hwang BY, Kim SJ, Lee SW, Lee HE, Lee CK, Hunter DJ, Jung KA (2012) Risk factors for medial meniscus posterior root tear. Am J Sports Med 40:1606–1610
12. Johannsen AM, Civitarese DM, Padalecki JR, Goldsmith MT, Wijdicks CA, LaPrade RF (2012) Qualitative and quantitative anatomic analysis of the posterior root attachments of the medial and lateral menisci. Am J Sports Med 40:2342–2347
13. Johnson DL, Swenson TM, Livesay GA, Aizawa H, Fu FH, Harner CD (1995) Insertion-site anatomy of the human menisci: gross, arthroscopic, and topographical anatomy as a basis for meniscal transplantation. Arthroscopy 11:386–394
14. Kohn D, Moreno B (1995) Meniscus insertion anatomy as a basis for meniscus replacement: a morphological cadaveric study. Arthroscopy 11:96–103
15. Krause WR, Pope MH, Johnson RJ, Wilder DG (1976) Mechanical changes in the knee after meniscectomy. J Bone Joint Surg Am 58:599–604
16. Kurosawa H, Fukubayashi T, Nakajima H (1980) Load-bearing mode of the knee joint: physical behavior of the knee joint with or without menisci. Clin Orthop Relat Res 149:283–290
17. LaPrade CM, Jansson KS, Dornan G, Smith SD, Wijdicks CA, LaPrade RF (2014) Altered tibiofemoral contact mechanics due to lateral meniscus posterior horn root avulsions and radial tears can be restored with in situ pull-out suture repairs. J Bone Joint Surg Am 96:471–479
18. Maquet PG, Van de Berg AJ, Simonet JC (1975) Femorotibial weight-bearing areas. Experimental determination. J Bone Joint Surg Am 57:766–771
19. Marzo JM, Gurske-DePerio J (2009) Effects of medial meniscus posterior horn avulsion and repair on tibiofemoral contact area and peak contact pressure with clinical implications. Am J Sports Med 37:124–129
20. Moulton SG, Bhatia S, Civitarese DM, Frank RM, Dean CS, LaPrade RF (2016) Surgical techniques and outcomes of repairing meniscal radial tears: a systematic review. Arthroscopy 32:1919–1925
21. Pache S, Aman ZS, Kennedy M, Nakama GY, Moatshe G, Ziegler C, LaPrade RF (2018) Meniscal root tears: current concepts review. Arch Bone Joint Surg 6:250–259
22. Packer JD, Rodeo SA (2009) Meniscal allograft transplantation. Clin Sports Med 28:259–283
23. Petersen W, Tillmann B (1998) Collagenous fibril texture of the human knee joint menisci. Anat Embryol (Berl) 197:317–324
24. Saigo T, Tajima G, Kikuchi S, Yan J, Maruyama M, Sugawara A, Doita M (2017) Morphology of the insertions of the superficial medial collateral ligament and posterior oblique ligament using 3-dimensional tomography: a cadaveric study. Arthroscopy 33:400–407
25. Schillhammer CK, Werner FW, Scuderi MG, Cannizzaro JP (2012) Repair of lateral meniscus posterior horn detachment lesions: a biomechanical evaluation. Am J Sports Med 40:2604–2609
26. Seedhom BB, Dowson D, Wright V (1974) Proceedings: functions of the menisci. A preliminary study. Ann Rheum Dis 33:111
27. Sheps DM, Otto D, Fernhout M (2005) The anatomic characteristics of the tibial insertion of the posterior cruciate ligament. Arthroscopy 21:820–825
28. Stärke C, Kopf S, Gröbel K-H, Becker R (2010) The effect of a nonanatomic repair of the meniscal horn attachment on meniscal tension: a biomechanical study. Arthroscopy 26:358–365
29. Tajima G, Nozaki M, Iriuchishima T, Ingham SJ, Shen W, Smolinski P, Fu FH (2009) Morphology of the tibial insertion of the posterior cruciate ligament. J Bone Joint Surg Am 91:859–866
30. van Trommel MF, Simonian PT, Potter HG, Wickiewicz TL (1998) Arthroscopic meniscal repair with fibrin clot of complete radial tears of the lateral meniscus in the avascular zone. Arthroscopy 14:360–365
31. Yamamoto M, Hirohata K (1991) Anatomical study on the menisco-femoral ligaments of the knee. Kobe J Med Sci 37:209–226

Publisher's Note Springer Nature remains neutral with regard to jurisdictional claims in published maps and institutional affiliations.